

In Vivo correlation between non-model-based parameters and model-based K_{tr} in brain tumors

C-F. Chen¹, L-W. Hsu², and H-L. Liu²

¹Department of Radiology, Chang Gung Memorial Hospital, Chiayi, Taiwan, Taiwan, ²Department of Medical Imaging and Radiological Sciences Institute of Medical Physics and Imaging Sci, Chang Gung University, Taoyuan, Taiwan, Taiwan

Introduction:

Recently, dynamic contrast-enhanced MRI (DCE-MRI) has been more and more widely applied in cancer diagnosis and treatment follow-up because of non-invasive and non-radiation. The most common estimated parameters in DCE-MRI are K^{tr} and V_e. These parameters which come from pharmacokinetic models could be surrogates of the real physiology. However, the process of K^{tr} estimation is not easy. The non-modeled parameter, such as IAUC, was often used owing to its advantages of avoiding some challenges associated with pharmacokinetic modeling. For overall application in the wide-ranged physiologic variations, a modified IAUC_{K^{tr}} (mIAUC_{K^{tr}}) was proposed by simulation [1]. In this study, we aim to further investigate the application of mIAUC_{K^{tr}} in clinical and find the correlation between mIAUC_{K^{tr}} and K^{tr}.

Materials and Methods:

Total 10 patients with brain tumors were participated in this study. Age ranged from 38 to 69 years (means=51±11.04 years) with 6 males and 4 females. DCE-MRI T1 weighted images in the axial plane were acquired by using a gradient-echo sequence with TR/TE/θ=5.8 msec/2.2 msec/30° by a 3 Tesla scanner. The bolus injection of 0.1 mmol/kg gadolinium agent was administered through the antecubital vein by the power injector. Four parameters were utilized in this study: K^{tr}, IAUC_s, IAUC_c, and mIAUC_{K^{tr}}. K^{tr} were calculated according to the TK model [2]. IAUC_s and IAUC_c are the integral of signal time curve and the integral of concentration time curve during t1 (time point of contrast medium arrival) to t2 (the last time point within 60 seconds after contrast medium arrival), respectively. mIAUC_{K^{tr}} derived from the “curvature” of the vascular phase was calculated by the following equation:

$$mIAUC_{K^{tr}} = \left\{ \left[\frac{(IAUC_{60}/IAUC_{REF60})^{1.15}}{IAUC_{60-80}/2} \right] \times (IAUC_{180-300}/2)^{0.49} - 0.9 \frac{IAUC_{20}}{IAUC_{REF20}} \right\}^{1.9}$$

The statistical correlations between K^{tr}, IAUC_s, IAUC_c, and mIAUC_{K^{tr}} were processed with Matlab.

Results:

Figure 1 showed the maps of K^{tr}, IAUC_s, IAUC_c, and mIAUC_{K^{tr}} from patient No.1 with anaplastic oligodendroglioma. As the map displayed, the maximum mIAUC_{K^{tr}} was found in the right frontal lesion, as the result from the map of K^{tr}. The relationship between K^{tr} and IAUC_s, K^{tr} and IAUC_c, and K^{tr} and mIAUC_{K^{tr}} were displayed in Figure 2. The correlation coefficients between these non-modeled parameters and K^{tr} were 0.88, 0.92, and 0.95, respectively. With the p-value of 0.003, mIAUC_{K^{tr}} was significantly more correlated with K^{tr} than the others.

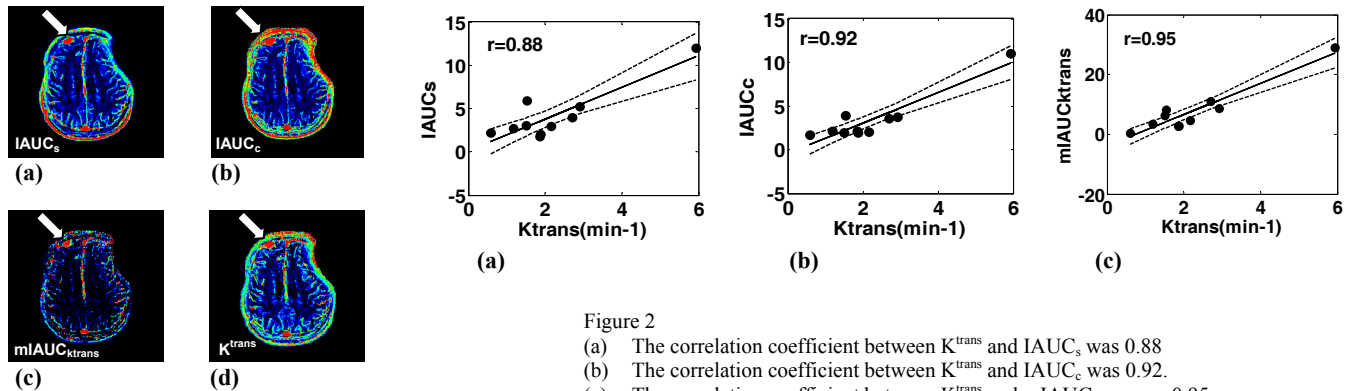


Figure 2

- (a) The correlation coefficient between K^{tr} and IAUC_s was 0.88
 - (b) The correlation coefficient between K^{tr} and IAUC_c was 0.92.
 - (c) The correlation coefficient between K^{tr} and mIAUC_{K^{tr}} was 0.95
- With the p-value of 0.003, mIAUC_{K^{tr}} was most correlated with K^{tr}.

Figure 1

The maps of IAUC_s, IAUC_c, mIAUC_{K^{tr}} and K^{tr} were illustrated in (a),(b),(c),(d), respectively. The arrow indicated the location of the lesion. Both maximum mIAUC_{K^{tr}} and K^{tr} were found in the lesion.

Discussion and Conclusions:

The feasibility of mIAUC_{K^{tr}} applied in brain tumors was successfully demonstrated in this study. The advantages of the mIAUC_{K^{tr}} are easy-practiced in clinical usage and arterial input function (AIF) free. On the other hand, the AIF selection is one shortcoming for K^{tr} calculation. Since the high correlation between K^{tr} and mIAUC_{K^{tr}} was demonstrated in this study, it reveals that mIAUC_{K^{tr}} could be an alternative for physiological condition evaluation in DCE-MRI.

References:

1. Cheng, H.L., *J Magn Reson Imag* 2009; 30: 864-872
2. Tofts, P.S. et al. *J Magn Reson Imag* 1997; 7: 91-101